Beam steering using optical parametric amplification in Kerr medium: a space-time analogy of parametric slow-light

Gil Fanjoux,* Eric Lantz, Jérémy Michaud, and Thibaut Sylvestre

Institut FEMTO-ST, Département d'Optique P. M. Duffieux, Université de Franche-Comté, CNRS UMR 6174, 25030 Besançon, France

*gil.fanjoux@univ-fcomte.fr

Abstract: In a way analogous to a light pulse that can be optically delayed via slow light propagation in Kerr-type nonlinear media, we theoretically demonstrate that beam steering and spatial walk-off compensation can be achieved in noncollinear optical parametric amplification. We identify this effect as a result of the quadratic phase shift induced by parametric amplification that leads to the cancellation of the spatial walk-off and collinear propagation of all beams though they have different wavevectors. Experimental evidence is reported of a soliton array steering in a Kerr slab waveguide.

© 2012 Optical Society of America

References and links

1. L. Thévenaz, "Slow and fast light in optical fibers," Nat. Photon. **2**, 474–481 (2008).
2. Y. Okawachi, M. S. Bigelow, J. E. Sharping, Z. Zhu, A. Schweinsberg, D. J. Gauthier, R. Boyd and A. Gaeta, "Tunable all-optical delays via Brillouin slow light in an optical fiber," Phys. Rev. Lett. **94**, 153902 (2005).
3. K. Y. Song, M. G. Herráez, and L. Thévenaz, "Observation of pulse delaying and advancement in optical fibers using stimulated Brillouin scattering," Opt. Express **13**, 82–88 (2005).
4. J.E. Sharping, Y. Okawachi, and A.L. Gaeta, "Wide bandwidth slow light using a Raman fiber amplifier," Opt. Express **13**, 6092–6098 (2005).
5. D. Dahan and G. Eisenstein, "Tunable all optical delay via slow and fast light propagation in a Raman-assisted fiber optical parametric amplifier: a route to all optical buffering," Opt. Express **13**, 6234–6249 (2005).
6. E. Shumakher, A. Willinger, R. Blit, D. Dahan, and G. Eisenstein, "Large tunable delay with low distortion of 10 Gbit/s data in a slow light system based on narrow band fiber parametric amplification," Opt. Express **14**, 8540–8545 (2006).
7. N. Nasser, G. Fanjoux, E. Lantz and T. Sylvestre, "Tunable optical delay using parametric amplification in highly birefringent optical fibers," J. Opt. Soc. Am. B **28**, 2352–2357 (2011).
8. M. Peccianti, C. Conti, G. Assanto, A. De Luca, and C. Umeton, "Routing of anisotropic spatial solitons and modulation instability in liquid crystals," Nature **432**, 733–737 (2004).
9. W. E. Torruellas, G. Assanto, B. L. Lawrence, R. A. Fuerst, and G. I. Stegeman, "All-optical switching by spatial walk-off compensation and solitary wave locking," Appl. Phys. Lett. **68**, 1449–1451 (1996).
10. L. Torner, W. E. Torruellas, G. I. Stegeman, and C. R. Menyuk, "Beam steering by $\chi^{(2)}$ trapping," Opt. Lett. **20**, 1952–1954 (1995).
11. R. L. Carman, R. Y. Chiao, and P. L. Kelley, "Observation of degenerate stimulated four-photon interaction and four-wave parametric amplification," Phys. Rev. Lett. **17**, 1281–1283 (1995).
12. A. Penzkofer and H. J. Lehmeier, "Theoretical investigation of noncollinear phase-matched parametric four-photon amplification of ultrashort light pulses in isotropic media," Opt. Quant. Electron. **25**, 815–844 (1993).

13. M. Kauranen, A. L. Gaeta, and C. J. McKinstrie, "Transverse instabilities of two intersecting laser beams in a nonlinear Kerr medium," J. Opt. Soc. Am. B **10**, 2298–2305 (1993).
14. R. Malendevich, L. Jankovic, G. Stegeman, and J. S. Aitchison, "Spatial modulation instability in a Kerr slab waveguide," Opt. Lett. 26, 1879–1881 (2001).
15. C. Cambournac, H. Maillotte, E. Lantz, J. Dudley, and M. Chauvet, "Spatio-temporal behavior of periodic arrays of spatial solitons in a planar waveguide with relaxing Kerr nonlinearity," J. Opt. Soc. Am. B **19**, 574–585 (2002).
16. A. Dubietis, G. Tamosauskas, P. Polesana, G. Valiulis, H. Valtna, D. Faccio, P. Di Trapani, and A. Piskarskas, "Highly efficient four-wave parametric amplification in transparent bulk Kerr medium," Opt. Express **15**, 11126–11132 (2007).
17. G. P. Agrawal, *Nonlinear Fiber Optics*, 3rd ed. (Academic Press, 2001).
18. G. Fanjoux, J. Michaud, H. Maillotte, and T. Sylvestre, "Slow-light spatial soliton," Phys. Rev. Lett. **100**, 013908 (2008).

1. Introduction

Slow and fast light (SFL) has been the subject of numerous studies in fiber optics [1–5]. Among the various techniques, SFL has been achieved using optical parametric amplification (OPA) in a nonlinear optical fiber [5–7]. In such a process, OPA provides not only gain but also an optical delay between the interacting pulses that perfectly balances the temporal walk-off due to group-velocity dispersion (GVD) and leads to group-velocity matching between the interacting pulses [5, 7]. The present work aims to transpose this concept of all-optical control of group velocity to the spatial domain. Based on the well-known space-time duality of the nonlinear Schrödinger equation, we show that a laser beam can be significantly steered in a noncollinear spatial OPA interaction, in a way analogous to a light pulse that can be optically delayed through OPA. We provide a clear derivation of the formula for the phase shift and the spatial walk-off induced by OPA. It is also shown that this effect leads to spatial walk-off compensation and beam trapping, as previously shown in anisotropic liquid crystals [8] or quadratic media [9,10]. In this work, however, parametric beam steering and trapping is observed in isotropic Kerr media. Experimental evidence is reported of this remarkable behavior in soliton array generation by OPA in a Kerr planar waveguide. Note also that, since its first observation in 1996 [11], very few studies have focused on the spatial case of four-wave mixing in Kerr media [12–16], whereas temporal four-wave mixing or modulation instability processes have extensively been investigated in the context of fiber optics [17].

2. Theory

Let us consider the one-dimensional noncollinear spatial OPA interaction as that shown in Figs. 1(a) and 1(b). This degenerate four-wave mixing (FWM) involves an intense pump beam and two signal and idler weak beams with spatial angular frequency shifts from the pump of Ω and $-\Omega$, respectively. The three beams have the same wavelength λ and copropagate along a Kerr planar waveguide of length L. The pump beam is considered as a continuous wave in the free spatial transverse dimension x, whereas signal and idler beams have finite spatial width. Due to their different angular frequency, the signal and idler beams undergo opposite spatial walk-off X_L in the transverse dimension x with respect to the pump beam in linear regime, as schematically sketched in Fig. 1(b). This walk-off is given by the following simple analytical expression $X_L = \frac{\Omega}{\beta}L$, with $\beta = \frac{2\pi n_0}{\lambda}$ the wave vector, n_0 the refractive index of the medium, and L the propagation length. In nonlinear regime, the propagation of these three waves in a Kerr planar waveguide is governed by the (1+1)D nonlinear Schrödinger equation (NLSE) as

$$\frac{\partial A}{\partial z} = \frac{i}{2\beta}\frac{\partial^2 A}{\partial x^2} + i\gamma|A|^2 A, \tag{1}$$

where $\gamma = \frac{2\pi n_2}{\lambda}$ is the nonlinear coefficient and n_2 the nonlinear index. We then solved Eq. 1 by inserting the complex slowly varying amplitude of the form $A = \left(\sqrt{I} + A_s e^{i\Omega x} + A_i e^{-i\Omega x}\right) e^{i\gamma Iz}$, where $I = |A_p|^2$ is the pump intensity, A_s and A_i are the amplitudes of the signal and idler beams. In the undepleted pump regime, and after a reference change for the signal and idler phase as $B_{s,i} = A_{s,i} e^{-i\kappa z/2}$, we may write the following coupled amplitude equations as

$$\frac{\partial B_s}{\partial z} = i\gamma I B_i^* e^{-i\kappa z} \quad ; \quad \frac{\partial B_i}{\partial z} = i\gamma I B_s^* e^{-i\kappa z}, \tag{2}$$

where $\kappa = -\frac{\Omega^2}{\beta} + 2\gamma I$ is the phase mismatch including the linear and nonlinear phase shift. The complex OPA gain g_c for signal and idler beams can then be derived from these equations in the high gain regime as (for detailed calculations, see Ref. [7])

$$g_c = g - i\frac{\kappa}{2} \quad \text{with} \quad g^2 = (\gamma I)^2 - \left(\frac{\kappa}{2}\right)^2 \tag{3}$$

The real part of g_c acts on the field amplitudes and therefore provides the parametric gain g, whereas its imaginary part $-\frac{\kappa}{2} = \frac{\Omega^2}{2\beta} - \gamma I$ induces a spatial phase shift across the signal and idler beams that leads to a nonlinear spatial walk-off, like the time phase shift that induces an optical delay in the temporal OPA interaction [5]. By analogy with the parametric SFL theory [5], we may write the spatial group index variation Δn_{gx} and the induced spatial walk-off X_{NL} as

$$\Delta n_{gx} = -c\frac{\partial \Im m(g_c)}{\partial \Omega} \quad \text{and} \quad X_{NL} = \int_0^L \frac{\Delta n_{gx}}{c} dz \tag{4}$$

Using above expressions for g_c we find

$$\Delta n_{gx} = -c\frac{\Omega}{\beta} \quad \text{and} \quad X_{NL} = -\frac{\Omega}{\beta}L. \tag{5}$$

Note that the spatial group index n_{gx} is associated with the transverse beam velocity and does not correspond to the group index of the waveguide. Figure 1(c) shows the parametric gain g
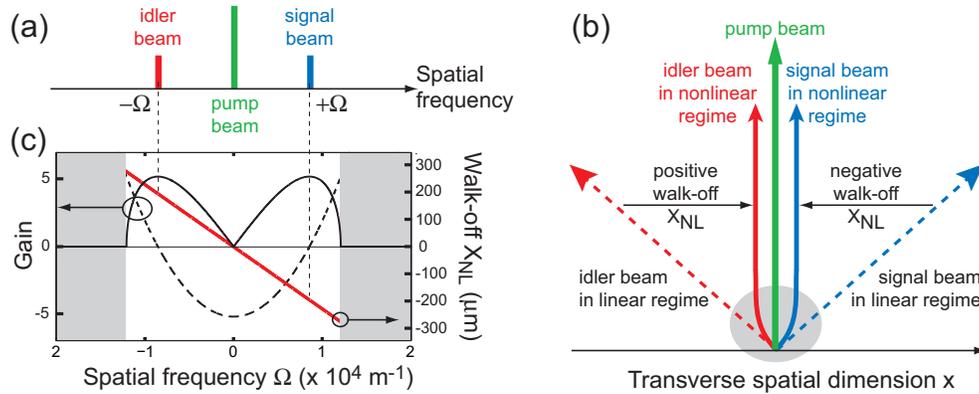

Fig. 1. (a) Spatial optical parametric amplification. (b) Scheme of the OPA-induced spatial walk-off compensation between the linear (dashed curves) and the nonlinear (solid curves) regime. (c) Real (black) and imaginary (dashed) parts of the complex parametric gain g_c versus the spatial frequency. Red curve shows the induced spatial walk-off. Parameters are the L=7cm, $\beta=1.9\times10^7 \text{m}^{-1}$, $\gamma = 4.10^{-11}$ m.W^{-1}, I $= 1.8\times10^{12}$ W.m^{-2}.

(solid curve) as a function of the spatial frequency, together with the imaginary part $\Im(g_c) = -\frac{\kappa}{2}$ as a dashed curve and the induced spatial walk-off X_{NL} in red, respectively. Parameters are listed in the caption of Fig. 1 and are those of a 7-cm long planar waveguide filled with carbon disulfide CS_2 as a nonlinear medium (for detailed parameters, see Refs. [15,18]). Figure 1(c) and Eq. (5) show that the signal and idler beams exhibit a nonlinear spatial walk-off X_{NL} that perfectly balances the linear one, as $X_{NL} + X_L = 0$. Moreover, this walk-off cancellation is obtained whatever the z position in the waveguide is, and whatever the spatial frequency detuning Ω is. In other words, spatial walk-off compensation and beam trapping is achieved throughout the propagation and over the full gain bandwidth. This remarkable behavior is schematically sketched in Fig. 1(c) that shows the beam propagation direction in the linear and nonlinear regime, respectively. When parametric amplification enters into play, the spatial walk-off is cancelled and all beams collinearly propagate despite their different wavevectors. This beam trapping effect is fully analogous to the group-velocity locking observed in the time domain [7]. We must also stress that it is not associated with a Kerr-induced waveguide because the pump beam is considered as a broad extended beam and therefore it cannot trapped the signal and idler by cross-phase modulation. Beam trapping is obtained in the undepleted pump regime and only when the linear gain regime is reached, condition for the validity of Eq. (5). Consequently, for small gain, their is transient regime for which the compensation is not perfect, leading to a residual spatial walk-off between the signal and idler, as drawn in Fig. 1(c) (gray area). When phase matching is fullfilled, i.e. $\kappa = 0$, Eq. (5) can be rewrite in the form $X_{NL} = -\sqrt{\frac{\gamma I}{\beta}}L = -\sqrt{\frac{n_2 I}{n_0}}L$, thus showing that tunable spatial walk-off can be achieved by varying either the pump intensity or the propagation distance.

3. Numerical simulations

To verify our simple analytical predictions, we performed numerical simulations of the NLSE (Eq. 1) by considering as a nonlinear Kerr medium a 7-cm long planar waveguide filled with carbon disulfide CS_2 [18]. A cw pump laser beam at 532 nm with an infinite spatial width is injected at the input with both the signal and idler beams with a width of 330 μm (full width at half maximum, Gaussian shape). Their spatial frequencies are set by the phase-matching condition as $\Omega/2\pi = \sqrt{2\gamma I \beta}/2\pi = \pm 8508 \mathrm{m}^{-1}$. Figure 2(a) illustrates the input and output spectra, with the parametric gain band (red dotted curve). Due to their small spatial width of 330μm compared to the pump, the signal and idler spectral widths are equal to about 3000 m^{-1}. By comparing the input and output spectra, it is clear that the signal and idler waves are amplified with more than 30 dB gain, in good agreement with the analytical curve. This amplification oc-
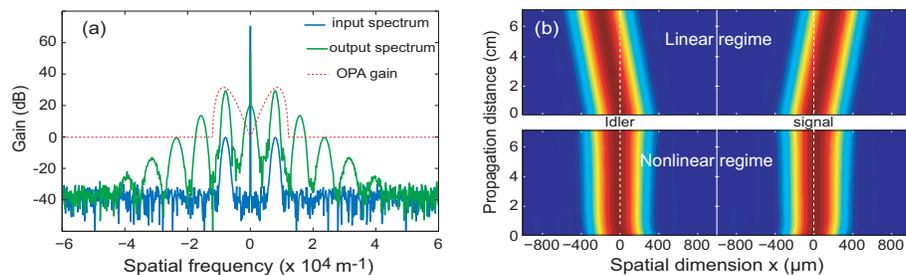

Fig. 2. Numerical simulations: (a) Input (blue) and output (green) parametric gain spectra and theoretical gain (red). (b) Normalized spatial intensity profiles versus propagation distance for signal and idler beams in the linear (pump off) and nonlinear (pump on) regime, respectively. Parameters are the same as in Fig. 1.
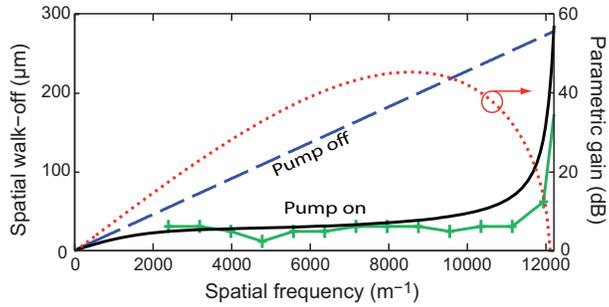
Fig. 3. Spatial walk-off versus the spatial frequency in the linear regime (pump off, dashed blue line) and in the nonlinear regime (pump on, black solid curve for analytical predictions and green curve for numerical results). Propagation length is L = 7 cm and pump intensity is I = 1.8×10^{12} W.m^{-2}. OPA gain band is also plotted a red dotted curve.

curs without any spectral shift, meaning that the walk-off variation is not associated to a wave vector change. By filtering the spectral components, the spatial evolution of signal and idler beams can be independently plotted along the propagation distance in the linear (pump off) and nonlinear (pump on) regime. As it can be seen in Fig. 2(b), in the linear regime, the two beams undergo an opposite spatial walk-off of 200μm, whereas in the nonlinear regime, both beams collinearly propagate without any walk-off, as predicted by our theory. A weak beam deviation at the beginning of the propagation can nevertheless be seen in Fig. 2(b), which is due to the fact that the steady linear gain regime is not fully established yet. In addition, our numerical simulations allowed us to check several behaviors. First, we have verified that after the waveguide signal and idler beams go back to their respective linear direction noncollinear to the pump, because their wavevectors have not been modified by OPA. Second, we also checked that, if the signal is out of the gain band, no walk-off compensation is observed, showing that this effect is not due to the XPM-induced phase shift. Finally, we also checked that the walk-off compensation is valid over the whole parametric gain band by tuning the signal frequency $\Omega/2\pi$. Figure 3 compares analytical predictions with numerical simulations of the spatial walk-off in linear (pump off, dashed blue line) and nonlinear regime (pump on, black solid curve for analytical predictions and green curve for numerical results), including the transient regime of low gain (integration of Eq. (4) for analytical results). The parametric gain band is also plotted in Fig. 3 in dotted red line for better understanding. As it can be seen, in the linear regime, the spatial walk-off linearly increases with the spatial frequency, whereas it is almost cancelled all over the gain band in the nonlinear regime up to the cutoff frequency. The residual spatial walk-off is due to the contribution of the transient regime for low gain at the beginning of the waveguide. Then the walk-off sharply increases beyond the gain band to recover its nominal value in the linear regime. The analytical curve (black) is in rather good agreement with the numerical simulations (green). An important condition must however be satisfied to cancel the walk-off by OPA. The signal and idler spectral width indeed has to be narrower than the gain bandwidth in order to avoid spectral filtering and beam spreading.

4. Simulation versus Experiment: Soliton array steering

In the following we will present some numerical simulations and experimental results showing beam steering by OPA in the case of spatial soliton array generation. As OPA is formally equivalent to induced modulation instability (MI), it leads in the spatial domain to the generation of soliton array in Kerr slab waveguide [14, 15]. We performed numerical simulations of soliton
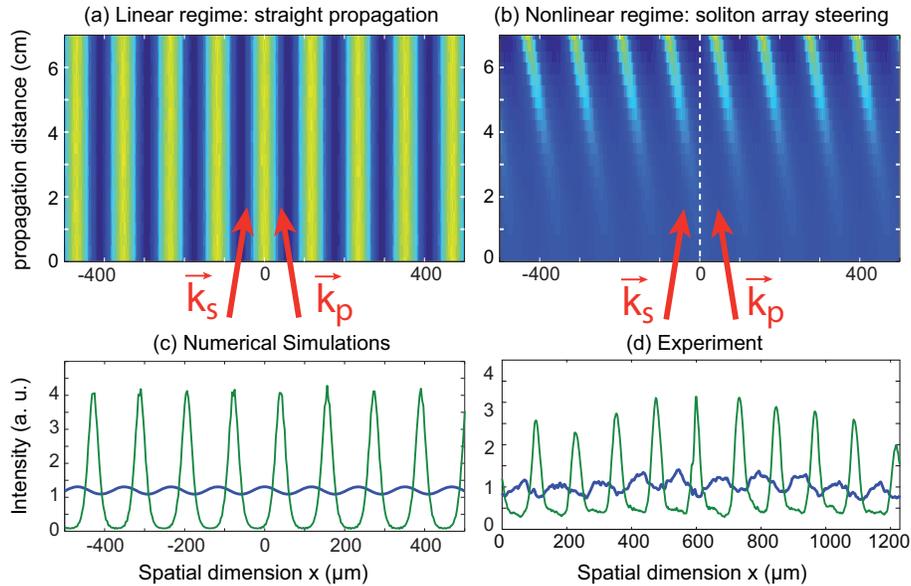
Fig. 4. Observation of soliton array steering by optical parametric amplification (after Ref. [15]). (a) Numerical simulations: straight propagation of the transverse modulation in the linear regime, $I = 1.2 \times 10^4$ W.m^{-2}. (b) Nonlinear regime: soliton array generation and steering by OPA, $I = 1.2 \times 10^{12}$ W.m^{-2}. (c) Numerical simulations: intensity profiles at the waveguide input (blue) and output (green). (d) Experimental observations. $\Omega/2\pi = 8550$m^{-1} and L=7cm.

array generation using the same experimental parameters as in Ref. [15]. We consider at the nonlinear waveguide input end a weak and broad signal beam frequency detuned by Ω from a strong pump beam. Here, pump and signal spatial frequencies are $+\Omega/2$ and $-\Omega/2$, as indicated by red arrows on Fig. 4. The two beams then combine into the waveguide and generate a weak transverse periodic modulation that propagates straightforward along the z direction, as shows the numerical simulation of Fig. 4 (a) for a low pump intensity. Figure 4(b) shows at a higher pump intensity the efficient generation of soliton array with clean sech shape, as shown by the intensity profiles plotted in Fig. 4(c). More importantly, we can see that the transverse soliton array is significantly steered at the output end of the waveguide by about one half period. This soliton steering can be immediately interpreted as a result of the nonlinear spatial walk-off induced by OPA. Since the signal beam will collinearly propagate to the pump all along the waveguide in the parametric gain regime, the soliton array undergoes a spatial walk-off which satisfies Eq. (5). Consequently, the output soliton array is spatially shifted from the input interference pattern. Figure 4(d) shows and compares the experimental intensity profiles recorded at our waveguide input and output ends, respectively (For details, See Ref. [15]). As it can be seen, the agreement with simulation is very good. We measure on Figs. 4(c,d) a spatial walk-off of 180 μm and a theoretical value from Eq. (5) of $X_{NL} = 200\mu$m.

5. Conclusion and Outlook

To resume, we theoretically demonstrated in isotropic Kerr media spatial walk-off compensation and beam steering in noncollinear optical parametric amplification. We have identified these remarkable effects as a result of the nonlinear spatial phase shift induced with the parametric gain. They are fully analogous to the optical delay generated in temporal OPA [5,7]. In

the spatial domain, parametric beam steering can find specific applications to simultaneously and all-optical amplification, ultrafast switching and routing of a weak signal beam by an intense pump beam. This result also suggests an interesting step towards the transverse control of laser beam in planar or bulk Kerr media where laser beams are known to be unstable and to collapse [16]. We will extend our (1+1)D NLSE model to higher dimensions including the (2+1)D case and the time domain. Finally, spatiotemporal parametric amplification in the short pulsed regime should also lead to simultaneous group-velocity and beam locking.

Acknowledgments